

Dynamic Instability of Liquidlike Motions in a Globular Protein Observed by Inelastic Neutron Scattering

W. Doster

Technische Universität München, D-8046 Garching, West Germany

S. Cusack

EMBL Grenoble Outstation, Institut Laue-Langevin, F-38042 Grenoble, France

W. Petry

Institut Laue-Langevin, F-38042 Grenoble, France

(Received 28 August 1989)

Inelastic neutron scattering was used to investigate liquidlike motions and the nature of a dynamical transition in myoglobin, a small globular protein. The signature of the transition is a strong enhancement of low-frequency density fluctuations and a corresponding decrease in elastic scattering above 180 K. It is shown that the line shape of the inelastic-scattering function approximates the scaling behavior predicted for a simple liquid by mode-coupling theories in the vicinity of the liquid-glass transition.

PACS numbers: 87.15.-v, 64.70.Pf

Globular proteins are polypeptide chains folded into densely packed spherelike structures (diameter 30–50 Å). Molecular-dynamic simulations of small proteins reveal similarities with atomic motions in other dense materials.^{1,2} Large atomic displacements are opposed by forces which stabilize the native structure leading to solidlike features at long times. However, since the packing is not as perfect as in molecular crystals, there is enough free volume to allow fast liquidlike motions. The limited degree of flexibility seems to be a prerequisite of biological function: The heme group of myoglobin, an oxygen storage protein in muscle tissue, is shielded from the solvent by the close-packed globin structure. Diffusion of dioxygen through the protein matrix and binding to the heme iron thus requires the assistance of density fluctuations.^{3–6} The liquid nature of these motions is emphasized by the observation of a freezing phenomenon, which resembles the liquid-glass transition of glass-forming liquids: The oxygen diffusion freezes in the vicinity of 200 K.⁷ Approaching 200 K from below, one observes an anomaly in the Lamb-Mössbauer factors of the heme iron^{8,9} and the protein protons,¹⁰ corresponding to enhanced atomic displacements. Mode softening of low-frequency vibrational modes¹¹ and, alternatively, stochastic dynamics describing activated transitions between conformational substates^{2,12–14} have been proposed as theoretical models.

The inelastic incoherent scattering of neutrons by protein protons allows us to probe both vibrational and diffusive motions. A first analysis of neutron-scattering experiments performed with hydrated myoglobin was neither consistent with mode softening nor with a simple stochastic description.¹⁰ Instead the spectra of myoglobin look very much like those obtained for glass-forming liquids.^{15–17} Such experiments were stimulated by recent mode-coupling theories (MCT) of the liquid-glass

transition.^{18–21} In this theory one considers density fluctuations as the most relevant low-frequency excitations in a liquid. The evolution of the density correlator is given by a damped oscillator equation with memory.²² The equation is closed by specifying the friction kernel again as a functional in the density correlator. The resulting nonlinear coupling of density modes enhances the effective friction and induces structural arrest at a critical temperature. Physically this approximates the back-flow phenomenon and the cage effect, describing concerted motions of particles in dense liquids.¹⁹ The theory treats correlations on a length scale of the interparticle distance, corresponding to density fluctuations whose wave vector is within the main peak of the static structure factor. MCT is thus a new microscopic model of the liquid-glass transition. It predicts scaling relations which are supported by recent neutron-scattering work on several liquids.^{15,16,23–26} To understand and to model the nature of density fluctuations in proteins it seems important to investigate whether the observed freezing phenomenon in myoglobin can be explained similarly by enhanced cage effects. We thus compare the line shape of inelastic-neutron-scattering spectra with scaling predictions of MCT. Consistency would support the concept of liquidlike motions and discrepancies could reveal protein-specific aspects.

The experiments were performed with D₂O-hydrated sperm-whale myoglobin (Sigma), $h = 0.36 \pm 0.04$ g/(g protein) to minimize solvent scattering (< 10%). Lyophilized material was exposed to a D₂O atmosphere, provided by a saturated KNO₃-D₂O solution.^{10,27} The procedure also exchanged the peptide hydrogen atoms (148 out of 1250) as judged from the infrared absorption band of the NH (ND) stretching vibration. The small amount of solvent (still comparable to the water content of crystals²⁷) suppresses rotational and translational

motion of the whole molecule, emphasizing internal fluctuations. It also ensures that the solvent contributes less than 10% to the scattering function even in the vicinity of the maximum in the static structure factor of D_2O at $Q=2.0 \text{ \AA}^{-1}$.

To cover a sufficient dynamic range the neutron-scattering experiments were performed using two spectrometers, the time-of-flight spectrometer IN6 and the backscattering instrument IN13 at the Institut Laue-Langevin in Grenoble. It was necessary to match the data points of the two spectrometers in the energy range where they overlap, 0.1–0.2 meV. In contrast to IN6, the IN13 data points scatter considerably in this energy range and have to be smoothed. However, the main results of the analysis are not strongly dependent on the precision of the match except possibly for the data set at 250 K (see below).

Figure 1(a) shows the scattering function $S(Q,E)$ derived from the time-of-flight spectrum of IN6 at various temperatures. To compensate for a harmonic temperature dependence, the spectra have been rescaled by the Bose factor to a common temperature of 180 K. No

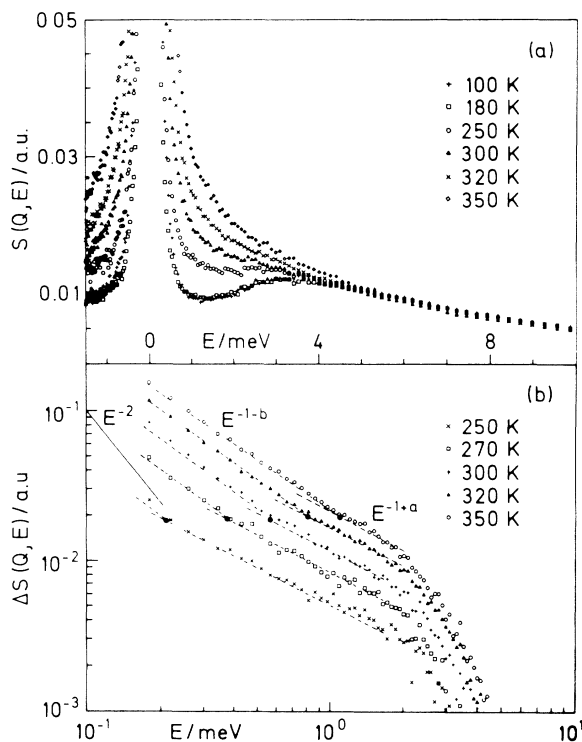


FIG. 1. (a) Dynamic structure factor $S(Q,E)$ at $Q=1.5 \text{ \AA}^{-1}$ (IN6) rescaled by the Bose factor to a common temperature of 180 K. (b) Excess dynamic structure factor; the dashed lines indicate the two power-law regions described in the text and the solid circles mark the crossover energy E_{\min} . Whether the elastic component was removed from the spectrum or not before the subtraction procedure had little effect on $\Delta S(Q,E)$ in the displayed energy range.

difference is observed between 100 and 180 K, the elastic peak being determined by the resolution of the instrument. The central peak broadens above 180 K in parallel with a nonlinear increase of the atomic mean-squared displacements.¹⁰ However, the inelastic spectrum above 3 meV is almost perfectly harmonic. Elsewhere, we show²⁸ that the peak near 3 meV marks the crossover from intermolecular acoustic modes (Debye continuum) to a weaker frequency dependence, characteristic of intramolecular protein vibrations. The low-frequency vibrations are breathing modes on a scale of the diameter of the molecule (40 \AA).²⁸ The anharmonic motions which broaden the central peak at the expense of the elastic component are most likely local segmental transitions.¹⁰ The different length scale and temperature behavior of harmonic and anharmonic motions suggests statistical independence. This allows us to subtract a harmonic vibrational background from $S(Q,E)$ at each temperature to analyze the anharmonic component. The difference spectrum $\Delta S(Q,E)$ is shown on a double-logarithmic scale in Fig. 1(b). $\Delta S(Q,E)$ is approximately Gaussian at the high-frequency end consistent with theoretical expectations, since a free flight leads to a Gaussian line shape. Moreover, the corresponding collision time, $\hbar/\Delta E (\approx 2 \text{ meV}) = 0.3 \text{ ps}$,¹⁰ is nearly temperature independent, supporting the validity of the subtraction procedure. The low-frequency spectrum may be approximated by two power laws, whereby the crossover energy decreases with temperature. The resulting exponent b [Fig. 1(b)] is definitely less than unity, which can be taken as the signature of a stretching phenomenon, typical for the primary structural relaxation of glass-forming liquids.²⁹ Further, the spectrum is not flat at higher energies, implying $a < 1$. This result is highly nontrivial because for Brownian motion one should expect a Lorentzian ($b=1$) on top of a flat, white-noise background ($a=1$). Such features are, however, derived within the framework of MCT.²⁰

The predicted behavior can best be observed in the imaginary part of the dynamic compressibility,^{15,30} defined as $\chi''(Q,E) = E\Delta S(Q,E)/kT$. This quantity should display a minimum characterizing the crossover between the two power laws in $\Delta S(Q,E)$. Further, the rescaled susceptibility $\hat{\chi}''(\hat{E}) = \chi''(Q,E/E_{\min})/\chi''(Q,E_{\min})$ in the vicinity of the minimum should be a temperature- and wave-vector-independent master function completely specified by the exponents a and b . The following interpolation formula has been proposed:²¹

$$\hat{\chi}''(\hat{E}) = (b\hat{E}^a + a\hat{E}^{-b})/(a+b), \quad E' < E < E_0. \quad (1)$$

E' and E_0 define the time scales of the primary process and the microscopic collisions, respectively. The exponents $0 < a < 0.5$, $0 < b < 1$ are solutions of the transcendental equation²¹ $\lambda = \Gamma^2(x+1)/\Gamma(2x+1)$, $x = -a$, $x = b$; $\Gamma(x)$ is the gamma function. The exponent parameter λ , $0.5 < \lambda < 1$, which contains reduced informa-

tion on the interaction potentials,³¹ specifies a and b and therefore χ'' in Eq. (1). In Fig. 2 we display the rescaled experimental data at 250 and 300 K, $Q=1.5 \text{ \AA}^{-1}$, and at 270 K, $Q=1.5$ and 2.0 \AA^{-1} . The data confirm the existence of a shape-invariant minimum in the susceptibility. Theoretical curves are shown for $\lambda=0.63$, 0.7, and 0.75. The shape of the minimum depends sensitively on λ and this restricts the possible parameter range despite the scatter in the data points. We obtain $\lambda=0.7 \pm 0.05$, which is comparable to Lennard-Jones (0.74) and hard-core liquids (0.76),³¹ and thus $a=0.33 \pm 0.05$, $b=0.64 \pm 0.1$.

In Fig. 3 we display the unscaled susceptibilities $\chi''(Q, E)$ at each temperature together with the theory, adjusting $\chi''(E_{\min})$ and E_{\min} . The spectra have been normalized to coincide at the high-energy end whose shape is temperature invariant. The figure also shows the theory convoluted with the resolution functions (dashed lines). Since the minimum of the spectrum at 250 K is located in the overlap region of the spectrometers ($E_{\min}=0.19 \text{ meV}$), we had to assume a scale factor determined at the higher temperatures to match the two data sets. The quality of the fit is quite reasonable except at the lowest temperature (220 K). As a consistency check we also adjust the exponents without constraints which leads to $a=0.41 (\pm 0.1)$, $b=0.55 (\pm 0.1)$ and somewhat smaller deviations (dotted lines). At 270 K the data taken at $Q=1.5$ and 2.0 \AA^{-1} demonstrate the approximate wave-vector independence of $\chi''(Q, E)$ excluding a significant distortion by coherent scattering of D_2O .

The signature of structural arrest is the slowing down of the primary component, resulting in a critical-temperature behavior of $\chi''(Q, E_{\min})$. The data of Fig. 3 now allow us to examine the scaling predictions concern-

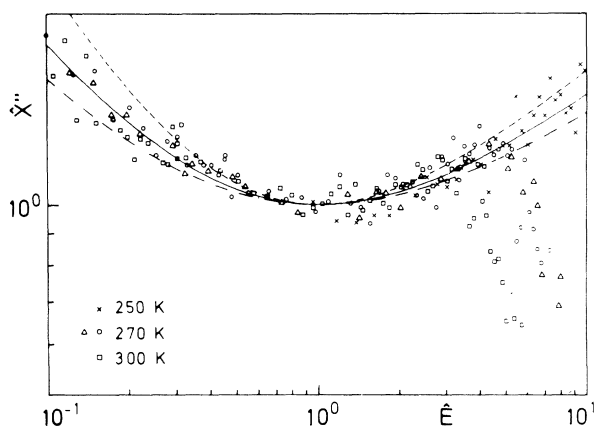


FIG. 2. Rescaled susceptibilities $\hat{\chi}''(\hat{E})$, experimental results combining data of IN6 and IN13 ($Q=1.5 \text{ \AA}^{-1}$). At 270 K, data at $Q=1.5$ (Δ) and 2.0 \AA^{-1} (\circ) are shown. Theoretical curves [Eqs. (1) and (2)] for $\lambda=0.75$ (---), 0.7 (—), and 0.63 (....) are also displayed.

ing the critical temperature T_c :²¹ $\chi''(Q, E_{\min}) \approx (T - T_c)^{0.5}$, $E_{\min} \approx (T - T_c)^{1/2a}$, combining the two equations gives $\chi''(Q, E_{\min}) \approx (E_{\min})^a$. The minima in Fig. 3 should thus be on a straight line with slope a (solid line). We obtain $a=0.36 \pm 0.1$ in reasonable agreement with $a=0.33$ derived from the shape of the spectrum. This implies that the two independent quantities $\chi''(E_{\min})$ and E_{\min} extrapolate to a common critical temperature. We find $T_c \approx 195 \pm 10 \text{ K}$, which is in the vicinity of the anomaly in the elastic scattering⁸⁻¹⁰ and the freezing of oxygen diffusion.⁷

MCT thus provides a consistent scenario using only two adjustable parameters, λ and T_c , to explain the complex temperature-dependent spectrum of myoglobin. The analysis also shows the potential of neutron scattering to test the predictions of MCT. Difficulties arise because of the necessity to use several spectrometers and to subtract a vibrational background. This can lead to spectral distortions. The failure to detect an obvious discrepancy between theory and experiment, surprising from a biologist's point of view, suggests that cage effects and not details in the force field dominate the average short-time behavior of protein dynamics. In fact, we have obtained quite similar data on lysozyme, a molecule with a quite different structure. The nonlinear feedback mechanism implied by MCT may allow us to understand how local fluctuations near an active site correlate with collective motions of the structure. The two kinds of displacements arise as two aspects of one nonlinear equa-

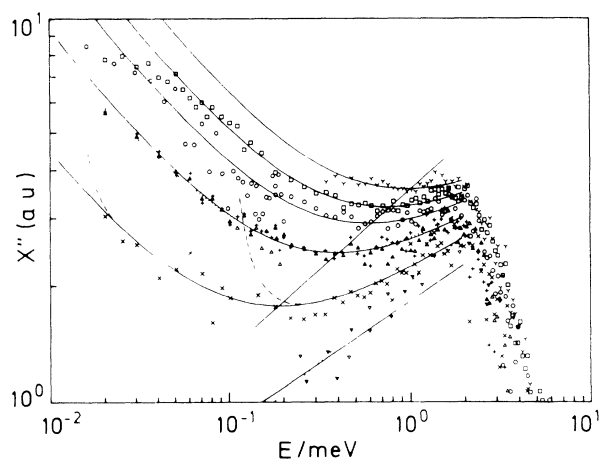


FIG. 3. Dynamic susceptibility at $Q=1.5 \text{ \AA}^{-1}$ at (Y) 350 K, (\square) 320 K, (\circ) 300 K, (Δ) 270 K, (\times) 250 K, (∇) 220 K, and (+) at $Q=2.0 \text{ \AA}^{-1}$ at 270 K. IN13 data cover the range 0.02–0.2 meV and IN6 data are shown above 0.15 meV. For clarity the spectra of the three lowest temperatures have been reduced by a factor of 0.9, which is evident at the high-energy end. Solid lines: theory, $\lambda=0.7$, $T_c=195 \text{ K}$; dotted lines at 220 and 270 K: Eq. (1) using $a=0.41$, $b=0.55$; dashed lines: Eq. (1) convoluted with the resolution functions of IN6 and IN13. The slope of the line connecting the minima is 0.41 instead of 0.36 as a result of the data reduction mentioned above.

tion of motion: The exponent $a < 1$ characterizes motions of particles coupled to the "heat bath" of nearest neighbors. The cage of nearest neighbors disintegrates at longer times in a self-similar cascade of less localized displacements (exponent b). The particle moves to a different cage. This process results in long-range diffusion which is arrested at the critical temperature. In a protein, long-range diffusion would violate the structural integrity, but the elementary step, escape of molecular groups out of the cage formed by their neighbors, is observed (rotation of side chains). The observed non-Gaussian Q dependence of the elastic incoherent structure factor¹⁰ indicates specific, asymmetric displacements in contrast to isotropic motions, expected for simple liquids. The protein structure thus controls the spatial distribution of displacements. Finally, the minimal achievement of the analysis may be, motivated but not biased by MCT, to expose otherwise unnoticed spectral features which can be compared to results of other methods such as molecular-dynamics simulations.³²

We thank Dr. A. Dianoux for assistance on IN6 and discussion of the manuscript. We are also grateful to Professor W. Götze, Dr. F. Fujara, and the late Professor E. Lüscher for many stimulating discussions.

¹J. A. McCammon, R. Gelin, and M. Karplus, *Nature (London)* **267**, 585 (1977).

²R. Elber and M. Karplus, *Science* **235**, 318 (1987).

³M. F. Perutz and F. S. Mathews, *J. Mol. Biol.* **21**, 199 (1966).

⁴D. A. Case and M. Karplus, *J. Mol. Biol.* **132**, 343 (1979).

⁵D. Beece, L. Eisenstein, H. Frauenfelder, D. Good, M. Marden, L. Reinisch, A. Reynolds, L. B. Sorensen, and K. T. Yue, *Biochem.* **19**, 5147 (1980).

⁶W. Doster, *Eur. Biophys. J.* **17**, 217 (1989).

⁷R. H. Austin, K. W. Beeson, L. Eisenstein, H. Frauenfelder, and I. C. Gunsalus, *Biochem.* **14**, 5355 (1975).

⁸F. Parak, E.W. Knapp, and D. Kucheida, *J. Mol. Biol.* **161**, 177 (1982).

⁹H. Keller and P. Debrunner, *Phys. Rev. Lett.* **45**, 68

(1980).

¹⁰W. Doster, S. Cusack, and W. Petry, *Nature (London)* **337**, 754 (1989).

¹¹W. Bialek and R. F. Goldstein, *Biophys. J.* **218**, 1027 (1985).

¹²E. W. Knapp, S. F. Fischer, and F. Parak, *J. Chem. Phys.* **78**, 4701 (1983).

¹³W. Nadler and K. Schulten, *Phys. Rev. Lett.* **57**, 1712 (1983).

¹⁴N. Agmon and J. J. Hopfield, *J. Chem. Phys.* **79**, 2042 (1983).

¹⁵W. Knaak, F. Mezei, and B. Farago, *Europhys. Lett.* **7**, 529 (1988).

¹⁶F. Fujara and W. Petry, *Europhys. Lett.* **4**, 921 (1987).

¹⁷B. Frick, in *Polymer Motion in Dense Systems*, edited by D. Richter and T. Springer, Springer Proceedings in Physics Vol. 29 (Springer-Verlag, Berlin, 1988), p. 143.

¹⁸W. Bengtzelius, W. Götze, and A. Sjölander, *J. Phys. C* **17**, 5915 (1984).

¹⁹W. Götze, *Phys. Scr.* **34**, 66 (1986).

²⁰W. Götze and L. Sjögren, in *Dynamics of Disordered Materials*, edited by D. Richter, A. J. Dianoux, W. Petry, and J. Teixeira, Springer Proceedings in Physics Vol. 37 (Springer-Verlag, New York, 1989), p. 18.

²¹W. Götze and L. Sjögren, *J. Phys. C* **21**, 3407 (1988).

²²E. Leutheusser, *Phys. Rev. A* **29**, 2765 (1983).

²³F. Mezei, W. Knaak, and B. Farago, *Phys. Rev. Lett.* **58**, 57 (1987).

²⁴F. Mezei, W. Knaak, and B. Farago, *Phys. Scr.* **19**, 363 (1987).

²⁵D. Richter, B. Frick, and B. Farago, *Phys. Rev. Lett.* **61**, 2465 (1988).

²⁶B. Frick and D. Richter, in *Dynamics of Disordered Materials* (Ref. 20), p. 38.

²⁷W. Doster, A. Bachleitner, R. Dunau, M. Hiebl, and E. Lüscher, *Biophys. J.* **50**, 213 (1986).

²⁸S. Cusack and W. Doster, *Biophys. J.* (to be published).

²⁹A. K. Jonscher, *Nature (London)* **267**, 673 (1977).

³⁰W. Doster, S. Cusack, and W. Petry, in *Dynamics of Disordered Materials* (Ref. 20), p. 120.

³¹J. L. Barrat, W. Götze, and A. Latz, *J. Phys. Condens. Matter* **1**, 7163 (1989).

³²J. Smith, K. Kuczera, and M. Karplus, *Proc. Natl. Acad. Sci. U.S.A.* **87**, 1601 (1990).